

American option pricing using generalised stochastic hybrid systems

Evelyn Buckwar^{*1}, Sascha Desmettre^{†2}, Agnes Mallinger^{‡3}, and Amira Meddah^{§1}

¹ Institute of Stochastics, Johannes Kepler University Linz,
Altenberger Straße 69, 4040 Linz, Austria

² Institute of Financial Mathematics and Applied Number Theory, Johannes Kepler University Linz,
Altenberger Straße 69, 4040 Linz, Austria

³ Linz School of Education, Johannes Kepler University Linz,
Altenberger Straße 69, 4040 Linz, Austria

September 27, 2024

Abstract

This paper presents a novel approach to pricing American options using piecewise diffusion Markov processes (PDifMPs), a type of generalised stochastic hybrid system that integrates continuous dynamics with discrete jump processes. Standard models often rely on constant drift and volatility assumptions, which limits their ability to accurately capture the complex and erratic nature of financial markets. By incorporating PDifMPs, our method accounts for sudden market fluctuations, providing a more realistic model of asset price dynamics. We benchmark our approach with the Longstaff-Schwartz algorithm, both in its original form and modified to include PDifMP asset price trajectories. Numerical simulations demonstrate that our PDifMP-based method not only provides a more accurate reflection of market behaviour but also offers practical advantages in terms of computational efficiency. The results suggest that PDifMPs can significantly improve the predictive accuracy of American options pricing by more closely aligning with the stochastic volatility and jumps observed in real financial markets.

Keywords— American options, option pricing, Piecewise Diffusion Markov Processes, stochastic hybrid systems, Longstaff-Schwartz algorithm.

1 Introduction

In the complex landscape of financial markets, the accurate pricing of American options plays a pivotal role, not just for theoretical analysis but also for practical portfolio management. American options grant holders the flexibility to exercise the option prior to its maturity, a feature that significantly influences cash flows and complicates their valuation due to stochastic volatility and the need for continuous dividend considerations.

^{*}Email: evelyn.buckwar@jku.at

[†]Email: sascha.desmettre@jku.at

[‡]Email: agnes.mallinger@jku.at

[§]Corresponding author: amira.meddah@jku.at

Traditional option pricing models, such as the Black-Scholes model, see [4], or the Merton model, see [27], have been cornerstones in understanding financial derivatives. These models provide key insights for risk management and decision-making processes, allowing traders and investors to estimate the value of options under a set of simplified assumptions. However, they typically assume constant drift rates and volatility, which fails to represent the inherent unpredictability of the market and its response to external shocks such as news, economic changes, or geopolitical events.

Over the last two decades, it has become clear that the assumption that the underlying asset's price behaves like a geometric Brownian motion with constant drift and constant volatility cannot explain the market prices of options with different strike prices and maturities. Merton [26] proposed adding jumps to the behavior of asset prices, which has led to active research into models with jumps. Several models have been proposed, including those by Kou [23] or Toivanen [31], which assume a log-double exponential distribution of jump sizes, and the Carr-Geman-Madan-Yor (CGMY) model [14], which treats the asset price as a Lévy process with possibly infinite jump activity. Another generalization involves stochastic volatility, as explored by Heston [19], among others. These developments aim to capture more accurately the complex dynamics of financial markets.

In order to incorporate these complexities into practical option pricing, several numerical methods have been developed. For instance, the binomial model has been enhanced by various researchers, including Cox et al. [16], Hull and White [20], and others, to capture the early exercise feature of options. However, these methods can be computationally intensive and memory-consuming. Similarly, Monte Carlo simulation approaches have been successful in generalizing option pricing [13, 18], although they have found limited use in scenarios involving early exercise [6, 8]. Furthermore, PDE methods have been notably advanced, using linear complementarity, front tracking, and front fixing methods to solve the free boundary problems associated with American options, see [7, 22, 1].

A widely used method for pricing American options is the Longstaff-Schwartz (LS) algorithm [24]. This method uses Monte Carlo simulations to generate multiple potential future paths of the underlying asset's price. The value of the American option is computed by averaging the discounted cash flows from these simulated paths. Further, the optimal exercise strategy is determined by a least-squares regression approach, which estimates the continuation values (expected future payoffs if the option is not exercised) at each potential exercise date. By regressing the continuation values against a set of basis functions of the underlying asset price, the algorithm approximates the decision to hold or exercise the option.

This paper introduces a novel approach by employing a generalised stochastic hybrid system for the pricing of American options, integrating continuous dynamics with jump processes to capture more realistic market fluctuations. Specifically, we use Piecewise Diffusion Markov Processes (PDifMPs), a type of generalised stochastic hybrid system, to model the asset price dynamics. PDifMPs combine the continuous evolution of asset prices with discrete jumps, allowing for sudden changes in market conditions, which are often triggered by unexpected events such as economic announcements or geopolitical developments.

Over the past decades, stochastic hybrid systems (SHS) have emerged as powerful modelling techniques in various fields, including mathematical biology [3, 15], neuroscience [29, 10], biochemistry [30], finance [21], to name a few. A prominent class of SHS, called piecewise deterministic Markov process (PDMP), was introduced by Davis in 1984 [17] and involves deterministic motion punctuated by random jumps. Building on this, Blom [5] proposed a more general model by incorporating stochastic differential equations (SDEs) and state-dependent reset maps, leading to the formulation of PDifMPs. This framework was further developed by Bujorianu et al. in [11], who established the theory and extended generators of PDifMPs.

Despite the applicability of generalised stochastic hybrid systems in various fields, including, for example, mathematical biology, [25, 28], to the best of our knowledge, they have not been applied to the context of American option pricing. The important role of PDifMPs in this work lies in their ability to model the stochastic nature of financial markets, capturing both continuous trends and abrupt shifts in asset prices. In our approach, we use PDifMPs to compute the asset price at various points in time. The possible exercise times for the American options are the jump times determined by the PDifMPs. At each of these jump times, we calculate the inner value of the option. We then discount

these inner values back to the present value using an appropriate discount factor. The option price is determined by taking the maximum of these inner values at the jump times, and then averaging these maximum values across all paths. Therefore, the final option price is obtained by averaging these discounted maximum values across all paths. This process is similar to the Longstaff-Schwartz algorithm in which we identify cash flows generated by the American put option at each jump time, discount these cash flows to time zero, and average them over all paths. However, instead of determining one optimal exercise time, we have the inner values at multiple stopping times.

The primary objective of this research is to improve the predictive accuracy of American option pricing by incorporating these advanced dynamics. By doing so, we aim to provide a model that aligns more closely with the erratic nature of financial markets, offering both theoretical insights and practical applications.

This paper is organized as follows: Section 2 provides a concise overview of PDifMPs and the foundational tools employed in this work. In Section 3, we introduce the mathematical framework of our proposed model, detailing the dynamic structure of asset price evolution. Section 4 explores the behavior of asset price paths through a series of numerical simulations. Section 5 focuses on American option pricing, where we present and compare results between two novel methods and the classic LS algorithm. Finally, Section 6 concludes with a summary of our findings and suggests potential directions for future research.

2 Fundamentals of PDifMPs

In this section, we present the fundamental concepts necessary for understanding PDifMPs. For a more complete overview, we refer the reader to [12, 11, 2].

2.1 Definition and notations

Consider a filtered probability space $(\Omega, \mathcal{F}, (\mathcal{F}_t)_{t \geq 0}, \mathbb{P})$, where the filtration $(\mathcal{F}_t)_{t \geq 0}$ is right-continuous and \mathcal{F}_0 contains all \mathbb{P} -null sets. Let $(W_t)_{t \in [0, T]} \in \mathbb{R}^m$, $m \in \mathbb{N}$, $T > 0$, represent a standard Wiener process defined on this space, and assume that W_t is \mathcal{F}_t -adapted.

Now, consider a PDifMP $(U_t)_{t \in [0, T]} = \{U(t, \omega) \mid t \in [0, T], \omega \in \Omega\}$, where $U_t = (S_t, \mu_t)$ takes values in $E = E_1 \times E_2$. Here, E_1 and E_2 are subsets of \mathbb{R}^d , $d \in \mathbb{N}$, both equipped with the Borel σ -algebra $\mathcal{B}(E)$. The set E is called the state space of the process U_t . The PDifMP $(U_t)_{t \in [0, T]}$ consists of two components such that

- The stochastic continuous component $(S_t)_{t \in [0, T]}$ has continuous paths in E_1 .
- The jump component $(\mu_t)_{t \in [0, T]}$ is a process with right-continuous paths and has piecewise constant values in E_2 .

The times at which the process μ_t undergoes a jump are denoted by $(T_i)_{i \in \mathbb{N}}$ and they form a sequence of random grid points within the interval $[0, T]$. Further, the dynamics of the PDifMP $(U_t)_{t \in [0, T]}$ on $(E, \mathcal{B}(E))$ are defined by its characteristic triple $(\phi, \lambda, \mathcal{Q})$ as follows.

Continuous dynamics

The stochastic flow $\phi : [0, T] \times E \rightarrow E_1$, $(t, u) \mapsto \phi(t, u)$ represents the solution of a sequence of SDEs driven by ν and σ , which are the drift and diffusion coefficients respectively:

$$\begin{cases} d\phi(t, u_i) = \nu(\phi(t, u_i), \mu_i)dt + \sigma(\phi(t, u_i), \mu_i)dW_t, & t \in [T_i, T_{i+1}), \\ \phi(T_i, u_i) = s_i. \end{cases} \quad (1)$$

Here, $u_i = (s_i, \mu_i)$ represents the newly updated state components at jump times T_i . At the endpoint T_{i+1} of each interval, s_{i+1} is set to the current value of $\phi(\cdot, u_i)$ to ensure the continuity of the path. Further, a new value μ_{i+1} is chosen as fixed parameter for the next interval according to the jump mechanism described below.

Jump Dynamics

The jump dynamics are governed by the rate function $\lambda : E \rightarrow \mathbb{R}_+$ and transition kernel $\mathcal{Q} : (E, \mathcal{B}(E)) \rightarrow [0, 1]$, determining the frequency at which the second component of $(U_t)_{t \in [0, T]}$ jumps and the new values of the second component after a jump occurs, respectively. The process $(U_t)_{t \in [0, T]}$ experiences jumps at times $(T_i)_{i \in \mathbb{N}}$ determined by the distribution of λ across the stochastic flow ϕ , given by

$$\mathcal{S}(t, u_i) = \exp\left(-\int_{T_i}^t \lambda(\phi(\delta, u_i), \mu_i) d\delta\right) \quad (2)$$

The function \mathcal{S} is called the survival function of the inter-jump times. This function states that there is no jump in the time interval $[T_i, t)$ conditional on the process being in the initial state u_i . The jump occurrences modify the state based on the transition probabilities specified by \mathcal{Q} . More precisely, let \mathcal{U} be a uniformly distributed random variable on $[0, 1]$, thus $\zeta : [0, 1] \times E \rightarrow \mathbb{R}_+$ is the generalised inverse of $\mathcal{S}(t, u_i)$ defined by

$$\zeta(\mathcal{U}, u_i) = \inf\{t \geq 0; \mathcal{S}(t, u_i) \leq \mathcal{U}\}. \quad (3)$$

Then there exists a measurable function $\psi : [0, 1] \times E \rightarrow E$ such that for $u_i \in E$ and $B \in \mathcal{B}(E)$

$$\mathbb{P}(\psi(\mathcal{U}, u_i) \in B) = \mathcal{Q}(u_i, B).$$

The function ψ represents the generalised inverse function of \mathcal{Q} . For a fixed t , $\psi(\mathcal{U}(\omega), U(\omega))$ is a random variable describing the post-jump locations of the second component of $(U_t)_{t \in [0, T]}$.

2.2 Iterative construction of PDifMP paths

The PDifMP $(U_t)_{t \in [0, T]}$ is constructed iteratively using its local characteristics $(\phi, \lambda, \mathcal{Q})$. Let $(\mathcal{U}_n)_{n \geq 1}$ be a sequence of iid random variables with uniform distribution on $[0, 1]$ and $u_0 = (s_0, \mu_0) \in E$ the initial value of (1) at $T_0 = 0$, such that u_0 can be either an \mathcal{F}_0 -measurable random variable (independent from the Wiener process) or a deterministic constant, for some $\omega \in \Omega$.

The survival function, defined in (2), is applied, along with its generalised inverse, defined in (3), to determine the first jump time of the second component. We proceed to define the sample path U_t up to the first jump time as follows:

$$\begin{cases} U_t = \phi(t, u_0) & \text{for } 0 \leq t < T_1, \\ U_{T_1} = \psi(\mathcal{U}_2, (\phi(T_1, u_0), \mu_0)). \end{cases}$$

The trajectory of U_t follows the stochastic flow ϕ given in (1) starting from $U_0 = u_0$ until a first jump occurs at the random time $t = T_1$. The post-jump state U_{T_1} is determined through the measurable function ψ . For all $B \in \mathcal{B}(E)$, the distribution of $\psi(\mathcal{U}_2, u_0)$ is given by

$$\mathbb{P}(\mu_{T_1} \in B | t = T_1, S_0 = s_0) = \mathcal{Q}((\phi(\tau_1, u_0), \mu_0), B), \quad (4)$$

where τ_1 is the waiting time until the first jump occurs, i.e., $\tau_1 = T_1$.

Restarting the process from the post-jump location U_{T_1} , we define

$$\tau_2 = \zeta(\mathcal{U}_3, U_{T_1})$$

as the next waiting time before a jump occurs from the survival function (2). In this way, we find the next jump time $T_2 = T_1 + \tau_2$.

Consequently, the state of the process in the interval $[T_1, T_2)$ is given by

$$\begin{cases} U_t = \phi(t - T_1, U_{T_1}) & \text{for } T_1 \leq t < T_2, \\ U_{T_2} = \psi(\mathcal{U}_3, (\phi(\tau_2, (U_{T_1}, \mu_0)), \mu_0)). \end{cases}$$

We proceed recursively to obtain a sequence of jump times $(T_i)_{i \geq 1}$,

$$T_i = T_{i-1} + \zeta(\mathcal{U}_{2i-1}, U_{T_{i-1}}) \quad \forall i \geq 1,$$

such that the generic sample path of U_t , for $t \in [T_i, T_{i+1})$, is defined accordingly by

$$\begin{cases} U_t = \phi(t - T_i, U_{T_i}) & \text{for } T_i \leq t < T_{i+1}, \\ U_{T_{i+1}} = \psi(\mathcal{U}_{2i+2}, (\phi(\tau_{i+1}, (U_{T_i}, \mu_{i+1})), \mu_{i+1})). \end{cases}$$

The number of jump times that occur between 0 and t is denoted by

$$N_t = \sum_{i \geq 1} \mathbb{1}_{(T_i \leq t)}.$$

This construction framework ensures that the sample path U_t is defined piecewise, with each segment determined by the dynamics prescribed by ϕ and the transitions to new states are dictated by \mathcal{Q} . The following assumptions ensure that the process is a strong càdlàg ¹ Markov process, guaranteeing the well-posedness of the model.

2.3 Assumptions

1. The functions $\nu : E \rightarrow \mathbb{R}^{d_1}$ and $\sigma : E \rightarrow \mathbb{R}^{d_1 \times m}$ are linearly bounded and globally Lipschitz continuous for all $s \in E_1$, ensuring the uniqueness solutions to the sequence of SDEs.
2. The jump rate function λ is measurable, such that the integral over any finite interval is finite, whereas over an unbounded interval, it is infinite, thus ensuring the existence of non-trivial dynamics.
3. The survival function and transition kernel are measurable and probabilistically well-defined, allowing for realistic modelling of jump occurrences.
4. For all $t > 0$ and for every starting point $u_i \in E$, $\mathbb{E}[N_t | u = u_i] < \infty$.

Having established the fundamental principles of PDifMPs, we now apply these concepts to the modelling of American options. Our approach unfolds in three structured steps to reflect market dynamics more accurately. Initially, we model the underlying asset with a time-varying drift, improving traditional models by better capturing market fluctuations. We then elaborate on how the asset price evolves using PDifMPs, integrating both continuous movements and discrete jumps that reflect real-world financial behaviors. Then, using this modelling approach, we identify the jump times of the PDifMP that are subsequently used as potential exercise times for American options. The following section provides a detailed explanation of these steps and their implications for option pricing.

3 Model Description: American options

American options are financial derivatives that provide the holder with the right, though not the obligation, to buy or sell an underlying asset at a predetermined price (the strike price) at any time prior to the expiration date of the option. This flexibility makes the valuation of American options a more intricate process in comparison to that of their European option counterparts, which can only be exercised at maturity T . Here, T is a positive and finite deterministic time.

The classical approach for modelling the price of the underlying asset is based on the Black-Scholes framework [4]. In this model, the drift rate of the underlying asset is assumed to be constant over

¹These are continuous-time stochastic processes with sample paths that are almost surely everywhere right continuous with limits from the left existing everywhere.

time, thereby suggesting a fixed expected rate of return throughout the asset's lifespan. Consequently, the asset price dynamics in the classical Black-Scholes model are described by the following SDE:

$$\begin{cases} dS_t &= \mu S_t dt + \sigma S_t dW_t \\ S(0) &= s_0, \end{cases} \quad t \in [0, T], \quad (5)$$

where μ is the constant drift rate, which we usually assume to be greater than the non-negative risk-free interest rate r , i.e., $\mu > r$. The risk-free interest rate r represents the rate of return of an investment with zero risk. In financial models, r is used to discount future cash flows to their present value, reflecting the time value of money.

Definition 3.1 (Discounting factor). *The discounting factor, which is used to determine the present value of future cash flows, given a constant interest rate r , is defined as follows*

$$D(t) = e^{-rt}, \quad t \in [0, T]. \quad (6)$$

In this context, the variable S_t represents the price of the underlying asset at time t , $t \in [0, T]$, with initial condition s_0 specifying the starting price of the asset. The term σS_t on the r.h.s of Equation (5) describes the exposure of the asset to market volatility, modeled as a function of the constant volatility parameter σ , $\sigma > 0$, associated to a standard Wiener process W_t .

The assumption of a constant drift rate in Equation (5) simplifies the complex dynamics of financial markets into a more manageable form, allowing, e.g., for deriving a closed-form solution for the price of a European option. However, in reality, asset prices can experience sudden changes due to various factors such as market news, earnings announcements, or changes in economic or political conditions. These elements can induce rapid and significant fluctuations in asset prices, thereby impacting the valuation of options and various derivative instruments.

Acknowledging the limitations of the constant drift assumption, we expand the Black-Scholes framework to encompass assets characterised by a variable drift rate. By integrating a time-varying drift into the model, we aim to capture a more realistic behaviour of asset returns that fluctuate in response to evolving market conditions. This approach allows for a more accurate reflection of market dynamics, accommodating the unpredictability and variability inherent in financial markets.

3.1 Modelling asset price dynamics with time-variant drift

Having established the essential elements of our extended model, we proceed to formulate the time-varying drift SDE that captures the behaviour of the asset prices as

$$\begin{cases} dS_t &= \mu_t S_t dt + \sigma S_t dW_t, \\ S(0) &= s_0. \end{cases} \quad (7)$$

In this formulation, the drift coefficient μ_t is subject to dynamic adjustment in order to reflect changing market conditions. It is an adapted stochastic process with respect to the filtration $(\mathcal{F}_t)_{t \in [0, T]}$, where the latter is generated by the Wiener process. We characterise μ_t as a jump process, defined as

$$\begin{cases} d\mu_t &= 0 dt, \\ \mu(0) &= \mu_0. \end{cases} \quad (8)$$

Here, μ_t takes piecewise constant values, changing only at discrete jump times T_i , $T_i < T$. More precisely, on each interval $[T_i, T_{i+1})$, $i = 1, \dots, n$, μ_t remains constant but may take different values across intervals, reflecting the occurrence of jumps. The mechanism by which the jumps occur and thus μ_t takes new values will be specified in the following section.

To model the asset price evolution under the influence of the dynamic drift, we assume that the sample path of an asset starting with value s_0 evolves according to SDE (7), influenced by the dynamic drift defined in Equation (8) for random periods. To describe this process, we rely on the PDifMP framework introduced in Section 2. We set $E_1 = \mathbb{R}$, $E_2 = \mathbb{R}_+$ and denote by $U_t := (S_t, \mu_t)$ the PDifMP

describing asset price dynamics. Here, the continuous process S_t and hence the process U_t are affected by spontaneous drift changes induced by the jump process μ_t . Thus, the state space of the piecewise process $U_t = (S_t, \mu_t)$ for asset price dynamics is $E = E_1 \times E_2$. The solution to the coupled system (7)-(8) is denoted by $\phi(t, U_t) := \phi(t, (S_t, \mu_t))$.

Throughout this paper, "jumps" represent sudden and significant changes in the price of the underlying asset, which can be either positive or negative. These jumps capture real-world scenarios where asset prices experience abrupt shifts due to market events. Moreover, the "jump times", correspond to the moments when these significant price changes occur and represent potential exercise dates for the American option. These times are particularly relevant when the price of the underlying asset is favourable - for example, when it exceeds the strike price of a call option - and thus influences the optimal exercise strategy.

3.2 Characterisation of the drift coefficient as a jump process

In this section, we focus on the PDifMP $U_t = (S_t, \mu_t)$ and define the jump mechanism of this process. Specifically, we detail the last two components of the characteristic triplet of the PDifMP U_t , namely the jump rate function λ and the transition kernel \mathcal{Q} , which together characterise the jump mechanism of the process. Indeed, the definition of the jump mechanism is crucial for capturing the exercise decisions of American options. These options introduce significant challenges in valuation and management due to the flexibility of early exercise, particularly when considering the optimal exercise timing based on evolving market conditions and the price performance of the underlying.

In our model, the jumps of the PDifMP U_t are governed by a non-homogeneous Poisson process with an intensity function $\lambda(U_t) := \lambda(S_t, \mu_t)$. This function allows the jump frequency to dynamically depend on both the current asset price and drift, reflecting the complex interplay between market conditions and strategic option holder decisions. More precisely, we choose

$$\lambda(U_t) := \lambda_0 + \eta \max(0, (|S_t - \delta| - \beta)), \quad t \in [0, T]. \quad (9)$$

Here, δ is a reference point for the asset price S_t around which the sensitivity of the jump rate $\lambda(U_t)$ is evaluated. Depending on the context, δ can be set to the strike price K , the initial asset price S_0 , or some other reference value. For instance, when δ is set to K , the model focuses on the deviation of the asset price from the strike price, which is important in assessing the moneyness of the option. When δ is set to S_0 , the model captures the volatility relative to the initial price of the asset. Therefore, δ could represent any specific threshold or benchmark around which the sensitivity of the jump rate is evaluated.

The parameter λ_0 represents the minimum intensity or frequency at which jumps in μ_t will occur under normal conditions. Essentially, λ_0 reflects the inherent volatility or instability of the market conditions surrounding the asset, independent of extreme price movements. This could be seen as capturing the background noise of the market, i.e. frequent but smaller shifts in market dynamics that are always present, even when no significant market events are driving significant changes.

Further, the role of the parameters β and η is to control how sensitive the jump rate is to changes in the asset price relative to the reference point δ . More specifically, β acts as a buffer zone around δ . This means that within the buffer zone ($|S_t - \delta| \leq \beta$), the jump rate remains at its baseline level λ_0 , reflecting normal market activity where small fluctuations in the asset price near δ are unlikely to trigger significant changes. However, outside the buffer zone ($|S_t - \delta| > \beta$), the jump rate begins to increase with distance from δ , reflecting increased market sensitivity and activity. As the asset price moves further away from δ , the probability of significant market events increases, potentially influencing decisions such as the exercise of options. This increase in jump rate is scaled by the parameter η .

In this context, η acts as a scaling factor that adjusts the jump intensity function $\lambda(U_t)$, directly affecting how the jump rate responds to deviations in the asset price S_t from δ . In particular, once S_t exceeds the buffer β , each unit of price deviation increases the jump rate by η . Higher η values increase the sensitivity of the jump rate, making the model highly responsive in volatile markets where stock prices are prone to dramatic shifts. This responsiveness allows the model to adapt rapidly to changes,

reflecting the rapid actions of market participants. Conversely, a lower η reduces the sensitivity of the model, stabilising the jump rate in less volatile markets where price changes are gradual and predictable, preventing overreactions to minor fluctuations and better suited to environments with less reactive market behaviour.

We now introduce the transition kernel \mathcal{Q} of the process U_t which, together with the jump rate λ , define the jump mechanism of the process. In particular, we employ the Laplace distribution as the probability density function for the drift dependent on the current state of the asset S_t , given by

$$\mathcal{Q}(U_t) := f(\mu|a(S_t), b) = \frac{1}{2b} \exp\left(-\frac{|\mu - a(S_t)|}{b}\right), \quad (10)$$

where

$$a(S_t) = \mu_0 + \alpha(S_t - \delta). \quad (11)$$

Equation (11) acts as the location parameter dependent on the price of the asset. The parameter μ_0 serves as a baseline for the drift level, and $\alpha(S_t - \delta)$ adjusts this base level based on the deviation of asset price from δ . Moreover, α in Equation (11) is a scaling factor that determines how the expected drift level, μ_t , adjusts in response to changes in the asset price relative to the reference point δ . It quantifies the extent to which the drift is influenced by the asset price moving away from or towards δ . In practical terms, the parameter α helps financial analysts and traders predict how sensitive the drift (and thus the asset or option pricing) is to changes in the market environment, aiding in more informed strategic decisions.

Further, the parameter b in (10) denotes the scale parameter of the Laplace distribution capturing the dispersion around the mean location $a(S_t)$. In particular, the choice of b affects the sensitivity of the model to underlying market dynamics. For instance, in volatile markets, a larger b value might be appropriate to capture the wide variance in drift changes, whereas in more stable markets, a smaller value for b could suffice. Hence, when pricing options, the choice of b is important as it affects the valuation of risk and uncertainty in future returns, directly influencing pricing strategies and risk assessments.

The Laplace distribution, known for its peakedness and heavy tails compared to the normal distribution, is particularly adept at representing significant yet infrequent events that can heavily impact financial markets. Therefore, the choice of a Laplace distribution to model the jumps associated with the drift process μ_t captures the asymmetric nature of financial market responses to various types of news and the leverage effect, where volatility increases as prices decrease. The ability of this distribution to represent skewed outcomes facilitates a more realistic representation of market responses to shocks, allowing for potentially larger changes in μ_t depending on the relationship between S_t and δ . Furthermore, the heavy tails of the Laplace distribution accommodate the fat-tailed behaviour of financial returns, acknowledging the higher likelihood of extreme market movements.

Finally, using the definition of the survival function (2), it is possible to construct the sequence of jump times $(T_n)_{n \geq 1}$, with $T_n = \tau_1 + \dots + \tau_n$, for all $n \geq 1$ (and $T_0 = 0$ by convention), such that the process U_t describing the asset price characterised by a variable drift rate, is piecewise constructed on each interval $[T_i, T_{i+1})$, $i = 1, \dots, n$, via the characteristics $(\phi, \lambda, \mathcal{Q})$ given by

$$\begin{cases} \phi &= S_0 \exp\left((\mu_t - \frac{\sigma^2}{2})t + \sigma W_t\right), \\ \lambda &= \lambda_0 + \eta \max(0, (|S_t - \delta| - \beta)), \\ \mathcal{Q} &= \frac{1}{2b} \exp\left(-\frac{|\mu - a(S_t)|}{b}\right). \end{cases} \quad (12)$$

Here, ϕ is the solution of the coupled system (7)-(8) and μ_t is a piecewise constant over each interval of random length $T_{i+1} - T_i$. As proven in [12], under the assumptions given in Section 2.3, this construction leads to a càdlàg strong Markov process, describing in our context the behaviour a stock price under market fluctuations.

Therefore, the system describing the behaviour of a stock price under market fluctuations is thus a

system concatenated over all subsequent intervals $[T_i, T_{i+1})$, such that for all $t \in [T_i, T_{i+1})$, $i \geq 0$, we have

$$\begin{cases} dS_t &= \mu_t S_t dt + \sigma S_t dW_t, \\ d\mu_t &= 0dt, \end{cases} \quad (13)$$

with initial values at the jump time T_i given by the values of S_t at the endpoint of the previous interval and a new constant value for μ_t drawn from the transition kernel \mathcal{Q} . The overall process of concatenated solutions of (13) is a couple $U_t = (S_t, \mu_t) \in E$, with $E = \mathbb{R} \times \mathbb{R}_+$.

4 Investigation of the asset price paths

Understanding the evolution of asset prices over time is crucial for accurately pricing options and managing financial risk. In this section, we explore the dynamics of asset price movements using a PDifMP model that incorporates jump processes to capture sudden market shifts. The PDifMP model extends traditional approaches by allowing for time-varying drift and jump intensity, providing a more flexible and realistic framework for modelling asset prices.

The importance of this research lies in its potential to improve our understanding of how different market conditions and model parameters affect the behaviour of asset prices. By examining the interplay between the baseline jump intensity λ_0 , the sensitivity parameter η and the initial asset price S_0 , we aim to gain insights into how these factors influence price paths, volatility and the frequency of significant market movements.

This section is structured around a series of numerical experiments designed to explore the effects of these parameters on asset price evolution. These experiments are essential to validate the PDifMP model's ability to simulate realistic asset price behaviour, particularly in comparison with traditional models such as Black-Scholes, which assume constant drift.

4.1 Numerical simulations

Let T be a fixed time horizon. In this section, we conduct a series of simulations of the PDifMP U_t , which models the evolution of the asset price as defined in (13). The purpose of these simulations is to examine the impact of the jump rate function on significant changes (both positive and negative) in the asset price. The simulation of the PDifMP U_t is based on the construction detailed in Section 2.2 and is carried out using a self-developed code in **R** (See Algorithm 1). For more details about the simulation of PDifMPs, we refer the reader to [9].

Algorithm 1 Asset price as PDifMP

Require: Intensity λ , maturity T , initial asset price S_0 .

- 1: Initialise vector S with S_0 .
 - 2: Initialise vector $jumpTimes$ with 0.
 - 3: Generate T_1 by the thinning method and rate λ and S_{new} until T_1 as a solution of the corresponding SDE.
 - 4: Set a counter $i = 1$.
 - 5: **while** $T_i < T$ **do**
 - 6: Append S_{new} to S .
 - 7: Append T_i to $jumpTimes$.
 - 8: Draw a new μ from the Laplace distribution.
 - 9: $i = i + 1$.
 - 10: Generate T_i by the thinning method with rate λ and simulate S_{new} until T_i as a solution of the corresponding SDE.
 - 11: **end while**
 - 12: Simulate S_{new} until T as a solution of the corresponding SDE.
 - 13: Append S_{new} to S .
 - 14: Append T to $jumpTimes$.
 - 15: Output S and jump times $jumpTimes$.
-

For this purpose, we first specify in Table 1 the parameters and coefficient involved in the simulation of the System (13). We now present a series of numerical experiments to obtain insight into several

Parameter	Description	Value (unit)
s_0	initial stock price	36 \$
λ_0	minimum frequency of fluctuation	0.01 – 50
η	sensitivity of fluctuation in $\lambda(U_t)$	0 – 1
K	strike price	40 \$
μ_0	initial drift	0.06
σ	diffusion coefficient	0.2
α	scaling factor	10^{-6}
b	scaling factor	0.01
β	buffer zone value	0

Table 1: **Model parameters.** Parameters used for simulating PDifMP asset prices.

features characterising the proposed approach. More precisely,

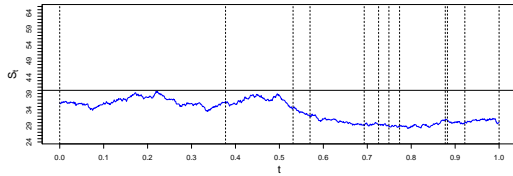
- (A) we consider the model for fixed values for λ_0 , α and b and we assess the effects of varying η on the stock price;
- (B) we consider the model for fixed values for η , α and b , and we evaluate the effects of the variation

of λ_0 on the stock price evolution and the potential exercise times.

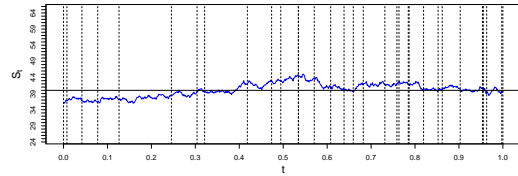
- (C) we fix the values of α and b and consider different combinations of λ_0 and η to show how their respective effects merge.

Starting with the numerical experiment (A), we examine the effects of varying η . This experiment is motivated by the need to understand the sensitivity of the stock price to changes in η , as it directly adjusts the responsiveness of the model to price deviations from the reference point δ , thereby influencing the overall dynamics of asset prices. We note that precise estimation of λ_0 , α and b can be difficult. As detailed in Section 3.2, λ_0 represents the baseline jump intensity, while α and b are scaling parameters in the Laplace distribution.

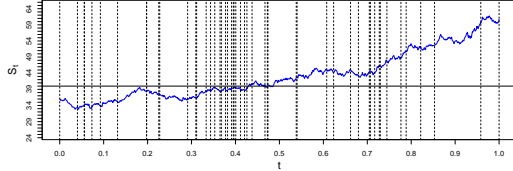
We fix $\lambda_0 = 5$; the remaining parameters are chosen as in Table 1, and we investigate the asset price evolution for different values of $\eta \in [0, 1]$.



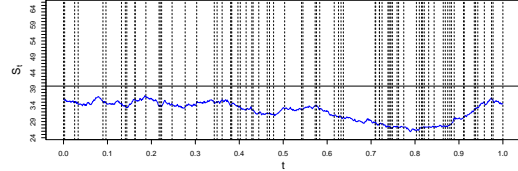
(a) Asset price evolution for $\eta = 0$.



(b) Asset price evolution for $\eta = 0.3$.



(c) Asset price evolution for $\eta = 0.5$.

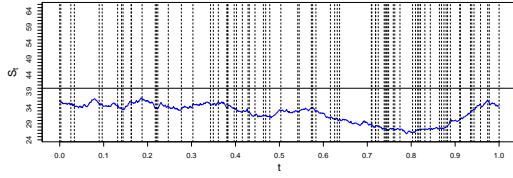


(d) Asset price evolution for $\eta = 1$.

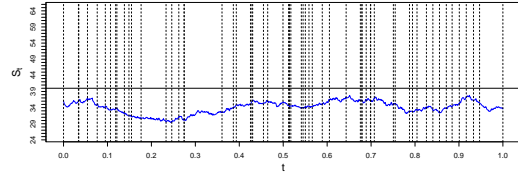
Figure 1: **Scenario (A)**. Numerical simulations of Equation (13) with the parameters listed in Table 1, $\lambda_0 = 5$ and for different values of η . The asset price evolution is shown after 1 year. The horizontal line represents the strike price.

In Figure 1, the plots illustrate the evolution of the asset price over a one-year period under different market sensitivities to price deviations from the initial asset price S_0 . In subplot (a), where $\eta = 0$, the asset price follows a relatively smooth trajectory with 12 jumps, indicating minimal sensitivity to deviations from S_0 . As η increases to 0.3 in subplot (b), the number of jumps increases to 32, leading to slightly more volatility, although the overall price path remains stable. Subplot (c) with $\eta = 0.5$ shows a further increase in sensitivity, resulting in 52 jumps and a more pronounced upward trend in the asset price. Finally, in subplot (d) with $\eta = 1$, the asset price shows 78 jumps, but the trend is less clear, with the path showing more frequent but not necessarily larger deviations from S_0 . This suggests that while η controls the frequency of jumps in the process, it does not directly affect the smoothness or volatility of the asset price path.

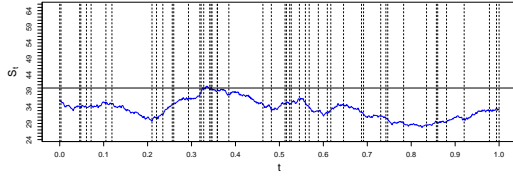
For the numerical test (B), we fix $\eta = 1$ and vary the value of the parameter λ_0 , which relates to the inherent volatility of the market conditions surrounding the asset. The results of the simulations for $\lambda_0 \in [0.01, 5]$ are shown in Figure 2.



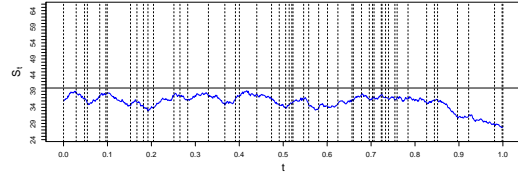
(a) Asset price evolution for $\lambda_0 = 5$.



(b) Asset price evolution for $\lambda_0 = 1$.



(c) Asset price evolution for $\lambda_0 = 0.1$.

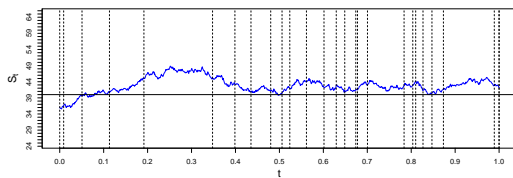


(d) Asset price evolution for $\lambda_0 = 0.01$.

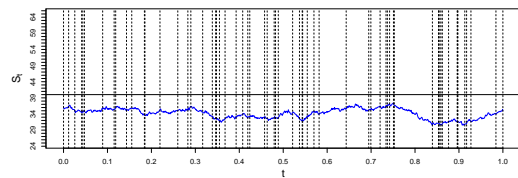
Figure 2: **Scenario (B)**. Numerical simulations of Equation (13) with the parameters listed in Table 1, here $\eta = 1$ is fixed, and we test for different values of η . The asset price evolution is shown after 1 year. The horizontal line represents the strike price.

The plots in Figure 2 show the asset price evolution over one year under varying baseline jump intensities. In subplot (a), where $\lambda_0 = 5$, the asset price exhibits significant volatility with 78 jumps. Subplot (b) with $\lambda_0 = 1$ shows a similar volatility pattern. As λ_0 decreases to 0.1 in subplot (c) and 0.01 in subplot (d), the asset price trajectories still display high volatility and 52 jumps. This indicates that for a high sensitivity parameter $\eta = 1$, changing the baseline jump intensity λ_0 does not significantly influence the volatility and frequency of jumps in the asset price. This occurs because the high value of η makes the jump intensity highly responsive to deviations in the asset price, overshadowing the effects of changes in λ_0 . Consequently, even with a lower λ_0 , the high η maintains substantial volatility due to its strong reaction to price deviations.

Referring to test (C), we analyse the interplay between the effects of the parameters λ_0 and η . In particular, we consider two different combinations $\eta = 0$, $\lambda_0 = 20$ and $\eta = 0.3$, $\lambda_0 = 50$. The results are shown in Figure 3.



(a) Asset price evolution for $\lambda_0 = 20$ and $\eta = 0$.



(b) Asset price evolution for $\lambda_0 = 50$ and $\eta = 0.3$.

Figure 3: **Scenario (C)**. Numerical simulations of Equation (13) with the parameters listed in Table 1. Here, we consider different values of η and λ_0 . The asset price evolution is shown after 1 year. The horizontal line represents the strike price.

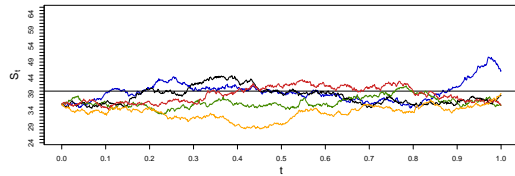
In Figure 3, we explore the asset price evolution over one year under two different scenarios: (a) with $\lambda_0 = 20$ and $\eta = 0$, and (b) with $\lambda_0 = 50$ and $\eta = 0.3$. In subplot (a), where the initial asset price is

set to 36 \$, the asset price shows a clear upward deviation from the initial value, reflecting a relatively smooth upward trend. In subplot (b), despite the higher λ_0 of 50 and a moderate $\eta = 0.3$, the asset price remains relatively stable and close to the initial value, without a significant upward or downward trend. Interestingly, while subplot (a) exhibits a positive trend, subplot (b) does not show increased volatility in terms of the asset price fluctuations compared to subplot (a). Instead, the main difference between the two scenarios lies in the number of jumps: subplot (b) has a higher frequency of jumps due to the increased λ_0 , which indicates more frequent but smaller adjustments to the asset price. This suggests that the increased jump rate in subplot (b) introduces more frequent corrections, keeping the asset price close to its initial value, while in subplot (a), the absence of jump sensitivity allows for a more pronounced deviation from the starting price.

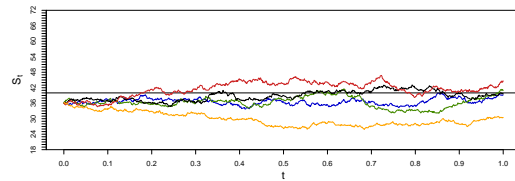
We now recall the jump rate function as detailed in (9), and we set $\delta = S_0$, the initial asset price, which allows us to examine the behaviour of the asset price under different initial conditions relative to the strike price.

To structure our analysis, we consider two primary scenarios based on initial values of S_0 : one where $S_0 = 36$, which is below the strike price, and another where $S_0 = 44$ \$, which is above the the strike price. For each of these scenarios, we conduct a series of numerical simulations to assess how the asset price evolves under different combinations of λ_0 and η . Hereafter, it is important to note that all the asset price paths in the following scenarios are generated using the same Wiener process, ensuring that variations in the paths are solely due to the differences in the parameters η and λ_0 . These scenarios are outlined as follows:

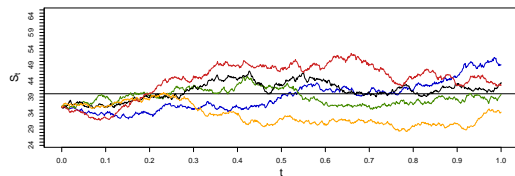
- (D) We examine the evolution of the asset price for an initial stock price $S_0 = 36$ \$, under various values of λ_0 and η to observe how the model responds when the initial price is below the strike price.
- (E) We repeat the analysis with an initial stock price $S_0 = 44$ \$, testing the same range of λ_0 and η values to compare how the price dynamics differ when the initial price is above the strike price.



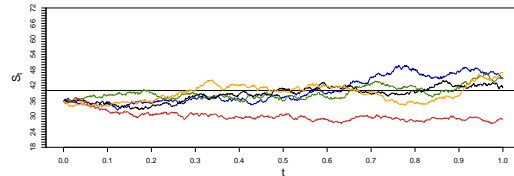
(a) Asset price evolution for initial $S_0 = 36$ and $\lambda_0 = 10$ and $\eta = 0$.



(b) Asset price evolution for initial $S_0 = 36$ and $\lambda_0 = 10$ and $\eta = 0.5$.



(c) Asset price evolution for initial $S_0 = 36$ and $\lambda_0 = 1$ and $\eta = 0.5$.



(d) Asset price evolution for initial $S_0 = 36$ and $\lambda_0 = 1$ and $\eta = 1$.

Figure 4: **Scenario (D)**. Numerical simulations of Equation (13) with the parameters listed in Table 1. Here, we fix the initial value of the stock price $S_0 = 36$ \$ for different values of η and λ_0 . The asset price evolution is shown after 1 year.

In the numerical test **(D)**, we examine the evolution of five asset price paths starting from an initial value $S_0 = 36$ \$, with different settings for the jump intensity parameter λ_0 and the sensitivity parameter η . The horizontal line indicates the strike price $K = 40$ \$. The results are shown in Figure 4. In subplot (a), where $\lambda_0 = 10$ and $\eta = 0$, the asset price paths appear relatively stable, with a slight upward trend for some paths, although most remain below the strike price $K = 40$ \$. The paths show limited fluctuations and, without sensitivity to deviations ($\eta = 0$), they do not appear to cluster tightly around the initial price $S_0 = 36$ \$.

Moreover, in subplot (b), where $\lambda_0 = 10$ and $\eta = 0.5$, the asset price paths show a more clustered pattern around the initial value $S_0 = 36$ \$. The introduction of some sensitivity ($\eta = 0.5$) tends to pull the paths closer to the initial value, although the overall spread seems to be slightly reduced compared to subplot (a). Furthermore, in subplot (c), where both $\lambda_0 = 1$ and $\eta = 0.5$, the asset price paths show what appears to be more significant upward movements compared to the previous plots. There appears to be an increasing divergence of the paths from the initial value $S_0 = 36$ \$, with some paths approaching or even exceeding the strike price $K = 40$ \$. This observation suggests that reducing λ_0 while keeping η moderate may increase the variability and upward movement of the paths.

Finally, in subplot (d), the asset price paths appear to be more tightly clustered for both $\lambda_0 = 1$ and $\eta = 1$ than in subplot (c), although there is still considerable variability. The higher sensitivity parameter $\eta = 1$ seems to cluster the paths more tightly, reducing the overall dispersion. However, there appears to be a less pronounced upward movement compared to subplot (c), suggesting that the increased sensitivity may moderate the magnitude of the deviation from the initial price. Overall, these observations suggest that η may control how tightly the paths are clustered around the initial value S_0 , while λ_0 seems to influence the overall trend and the magnitude of the deviation from this initial value.

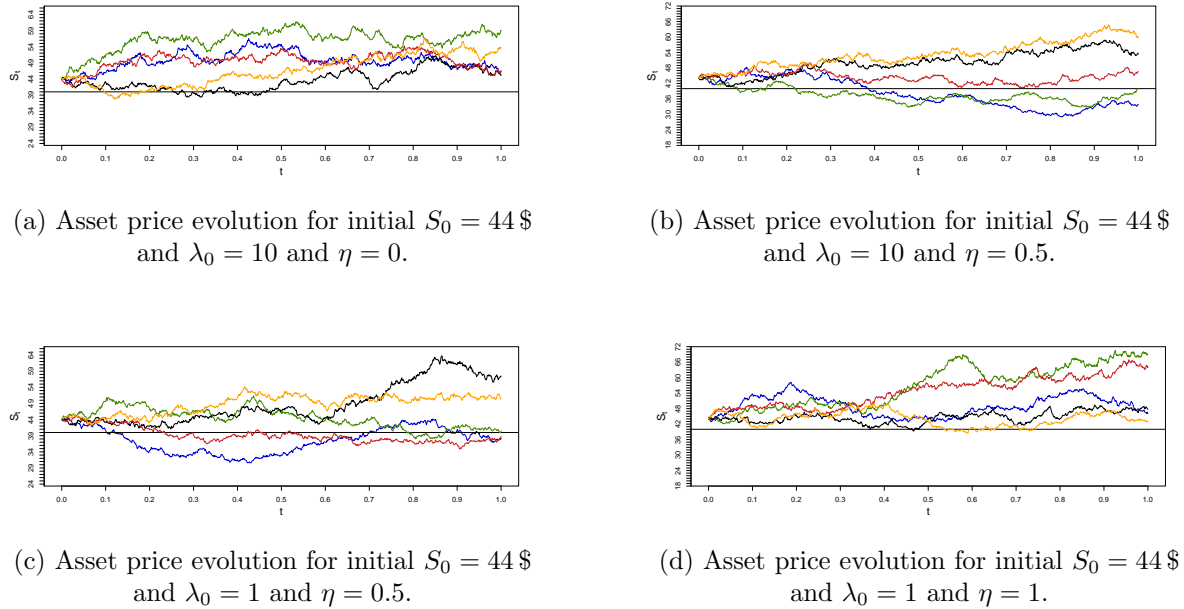


Figure 5: **Scenario (E)**. Numerical simulations of Equation (13) with the parameters listed in Table 1. Here, we fix the initial value of the stock price $S_t = 44$ \$ for different values of η and λ_0 . The asset price evolution is shown after 1 year.

In the numerical test **(E)**, we observe the evolution of five asset price paths, starting from an initial value of $S_0 = 44$ \$, with different settings for the jump intensity parameter λ_0 and the sensitivity parameter η . The horizontal line represents the strike price $K = 40$ \$, which is now lower than the initial asset price. The results are shown in Figure 5. In subplot (a), with $\lambda_0 = 10$ and $\eta = 0$, the asset

price paths appear to be relatively stable with limited fluctuations, showing an upward trend away from the strike price $K = 40$ \$. The paths appear clustered and gradually move upwards, suggesting that without sensitivity to deviations ($\eta = 0$), the asset price paths are less likely to deviate significantly from each other or from the initial value S_0 .

Introducing a moderate sensitivity, as shown in subplot (b), with $\eta = 0.5$ while keeping $\lambda_0 = 10$, the paths continue to show an upward trend, but with increased variability. The paths appear to cluster more closely around the initial value $S_0 = 44$ \$ compared to subplot (a), but with more pronounced deviations, both upwards and downwards. This suggests that adding some sensitivity to the model allows the paths to respond more dynamically to market conditions, although they still tend to be mostly above the strike price.

However, when both λ_0 and η are reduced to 1 and 0.5 respectively, as in subplot (c), the paths appear to show more varied behaviour, with some paths tending to move downwards and closer to the strike price. The increased sensitivity seems to lead to a wider spread between the paths, reflecting a greater divergence in their trajectories.

This behaviour seems to be more pronounced in subplot (d), where $\lambda_0 = 1$ and $\eta = 1$. Here, the asset price paths show a high degree of variability, with significant upward movements in some paths, which reach much higher levels than in the other subplots. The increased sensitivity to deviations due to the higher value of η seems to result in more pronounced divergences between the paths, with some moving sharply upwards and others showing less drastic changes. In conclusion, the numerical test **(E)** suggests that λ_0 and η play a crucial role in shaping asset price trajectories, especially when the initial price starts above the strike price.

We now compare the asset price paths generated by the PDifMP model to those produced by the geometric Brownian motion (GBM) model used in the Longstaff-Schwartz algorithm. The GBM model, which assumes a constant drift and volatility, is a standard approach in financial modelling for simulating the evolution of asset prices. In contrast, our PDifMP model incorporates a time-varying drift and jump intensity, making it more responsive to market conditions. By comparing these two approaches, we aim to highlight the differences in how each model captures the dynamics of asset prices, particularly under varying market conditions.

Figure 6 shows the evolution of asset prices over one year, simulated using the GMB model, which forms the basis of the LS algorithm. The initial conditions and volatility σ in this simulation are the same as those used in the PDifMP scenario **(D)**. The horizontal line indicates the strike price $K = 40$ \$. Unlike the PDifMP model, which incorporates a time-varying drift, the GBM model assumes a fixed drift rate. This results in smoother and more predictable asset price paths in the GBM model, highlighting the limitations of the constant drift assumption compared to the more dynamic and responsive PDifMP model, which better captures the complexity of market dynamics.

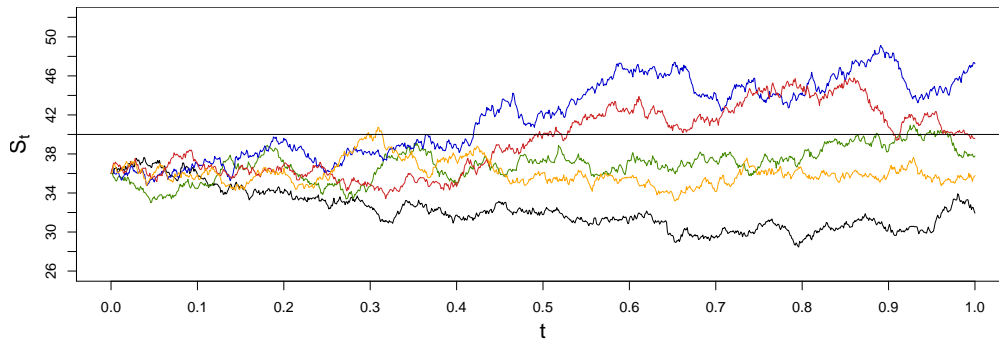


Figure 6: **Model comparison.** Asset price evolution simulated using the GMB model with the same initial conditions and σ values as in Scenario **(D)** and a constant drift. The evolution is shown after 1 year.

To provide a context for the next section, we present Figure 7, which illustrates the evolution of

asset prices computed using the PDifMP model with specific parameter values: $\lambda_0 = 0.6$, $\eta = 0$ and $\alpha = 0.01$. These values are representative of the parameters that will be examined in more detail in the following section. By examining this graph, we can observe the behaviour of the asset price under these conditions, including the number of jumps and the overall trend. This preliminary visualisation serves as a reference point for the more nuanced analysis to come, providing a glimpse of the dynamics that will be further explored with variations in these parameters. Moreover, the presence of fewer jumps in asset prices is consistent with real-world scenarios, where such jumps represent sudden deviations - either positive or negative - in asset prices. In reality, it is rare for a stock to experience significant trend changes more frequently than is the case here, making the output of this model a realistic approximation of typical market behaviour over the course of a year.

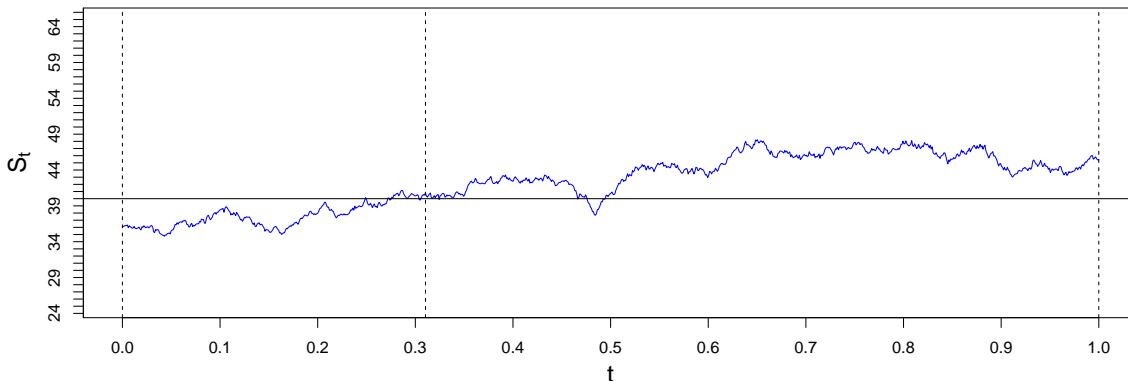


Figure 7: **Asset Price Evolution.** Asset price evolution computed using the PDifMP model with $\lambda_0 = 0.6$, $\eta = 0$, and $\alpha = 0.01$. The evolution is shown after 1 year.

5 Option pricing

Option pricing is a fundamental concept in financial mathematics, where the goal is to determine the fair value of an option — a financial derivative that grants the holder the right, but not the obligation, to buy (call option) or sell (put option) an underlying asset at a predetermined strike price K before or at a specified expiration date T . The flexibility of American options, which can be exercised at any time up to expiration, adds complexity to their pricing compared to European options, which can only be exercised at maturity.

The payoff of a call option at time $t \in [0, T]$ is given by $\max(S_t - K, 0)$, where S_t is the price of the underlying asset at time t . For a put option, the payoff is $\max(K - S_t, 0)$. When the payoff is positive, the option is said to be in the money.

This section compares three methods for pricing American options: the traditional Longstaff-Schwartz (LS) algorithm - which serves as a benchmark for the comparison - , a modified version of the LS algorithm using PDifMPs for asset price paths, and a novel approach that directly uses PDifMPs.

5.1 The Longstaff-Schwartz algorithm

The Longstaff-Schwartz algorithm, cf. [24], is a widely recognised method for pricing American options that require the determination of an optimal exercise strategy. The key challenge in pricing these options is to decide whether to exercise or continue to hold the option at each possible time, based on a comparison between the immediate exercise payoff and the expected future payoff from continuing to hold.

To address this, the Longstaff-Schwartz algorithm employs Monte Carlo simulations to generate multiple possible paths for the price of the underlying asset over the life of the option. By analysing these paths, the algorithm estimates the conditional expectation of the continuation value at each potential exercise date. This estimation is achieved through regression, where the continuation value is modelled as a function of the underlying asset price. The fitted regression model provides a direct estimate of the conditional expectation, which is then compared with the immediate exercise payoff to determine the optimal exercise strategy. The procedure is iterative, working backwards from the expiration date of the option to the first exercise date, thus allowing the value of the American option to be calculated. In more detail, the algorithm works as follows: Consider a series of simulated paths for the underlying asset S_t , where $t \in [0, T]$. The option can be exercised at a series of discrete times $0 < t_1 \leq t_2 \leq \dots \leq t_K = T$. The algorithm proceeds iteratively, starting from the last exercise date at maturity T . At each time step t_k , the decision to exercise the option is based on whether the option is "in the money" (i.e. where the payoff is positive). For each path where the option is in the money, the immediate exercise payoff is compared to the conditional expectation of the continuation value. This continuation value is estimated by regressing the discounted value of future cash flows Y on the current asset price X , using basis functions such as polynomials (e.g. linear, quadratic) or other functional forms such as Laguerre or Hermite polynomials.

Formally, let X represent the prices of the underlying asset at time t_k , and let Y denote the discounted value of subsequent option cash flows. The continuation value at time t_k is estimated as the conditional expectation $E[Y | X]$, obtained from the regression model. If the immediate exercise payoff exceeds the estimated continuation value, the optimal strategy is to exercise the option, setting the cash flow at time t_k to the immediate payoff and nullifying future cash flows for that path. Conversely, if the continuation value is higher, the cash flow at time t_k is set to zero, and the path continues.

This process is repeated for each exercise date, moving backwards in time until the first exercise date is reached. The final value of the option is then computed as the average of the discounted cash flows across all simulated paths.

In the LS algorithm, asset price dynamics are usually modelled using a geometric Brownian motion (GMB) characterised by constant drift μ and volatility σ . The simulation of these asset price paths is outlined in Algorithm 2.

Algorithm 2 Simulation of Sample Paths

Require: Maturity T , step size h , initial value S_0 , drift μ , and volatility σ .

- 1: Set $N = T/h$.
 - 2: Initialise a vector *path* of length $N + 1$.
 - 3: **for** $i = 1$ to N **do**
 - 4: Draw $\xi_i \sim \mathcal{N}(0, h)$, a normally distributed random variable with mean 0 and variance h .
 - 5: Update the $i + 1$ -th entry of *path* as $S_{i+1} = S_i \cdot \exp\left(\left(\mu - \frac{\sigma^2}{2}\right) \cdot h + \sigma \cdot \xi_i\right)$.
 - 6: **end for**
 - 7: Output the vector *path* containing the simulated asset prices.
-

Further, we detail below the implementation of the Longstaff-Schwartz algorithm specifically for put and call options. This algorithm uses the simulated asset price paths generated in the previous step to determine the option price, as outlined in Algorithm 3.

Parameter	Description	Value (unit)
S_0	initial stock price	36 – 44 \$
K	strike price	40\$
μ	drift rate	0.06
σ	volatility	0.2
h	step size	0.02
T	maturity	1 year
M	number of asset price paths	10000
M_E	number of exercise points	50

Table 2: **Model parameters.** Parameters used in the LS algorithm.

The simulation of sample paths and implementation of the Longstaff-Schwartz algorithm will use the parameters in Table 2 unless otherwise specified.

5.2 Longstaff-Schwartz algorithm with PDifMP-driven paths

We present here a modified version of the LS algorithm that incorporates PDifMPs into the asset price simulation, which we refer to as LS+PDifMP. Unlike the GBM model, PDifMPs combine continuous dynamics with discrete jumps, allowing them to more accurately model both gradual trends and sudden market shifts. By using PDifMP-generated paths instead of GBM, the LS+PDifMP approach can better reflect the time-varying nature of market conditions, especially in scenarios with significant volatility.

In this approach, the LS algorithm operates on asset price trajectories generated by PDifMPs that are influenced by the deviation of the asset from its initial value. This change is expected to increase the flexibility and accuracy of the model, allowing it to better capture the dynamic nature of market conditions. As a result, the LS+PDifMP approach has the potential to be a more effective tool for pricing American options, particularly in volatile markets. The simulation process is conducted by combining Algorithm 1, which generates PDifMP paths, with Algorithm 3, which applies the LS algorithm to these paths. Unless otherwise specified, the parameters listed in Table 3 will be used for these simulations.

Algorithm 3 Longstaff-Schwartz algorithm

Require: Maturity T . Matrix $paths$ with M rows (each representing a simulated asset price path) and M_E columns (each representing an exercise time), and the strike price K .

- 1: Initialise a matrix $cash_flows$ of size $M \times M_E$ with zeros.
 - 2: Set the last column of $cash_flows$ to the inner value for each path, i.e., $\max(K - paths[:, M_E], 0)$.
 - 3: **for** $t = M_E - 1$ to 2 (step backwards) **do**
 - 4: Set the vector X of asset prices at time t , i.e., $X = paths[:, t]$.
 - 5: Identify the paths where the option is in the money, i.e., $in_the_money = \{i : X[i] < K\}$.
 - 6: Extract the corresponding X values, $X_{in_the_money}$, and the discounted future cash flows $Y_{in_the_money}$ for these paths.
 - 7: Perform a regression of $Y_{in_the_money}$ on a constant, $X_{in_the_money}$, and $X_{in_the_money}^2$ to estimate the continuation value.
 - 8: Calculate the inner value vector $inner_value = K - X_{in_the_money}$.
 - 9: **for** $j = 1$ to $|in_the_money|$ **do**
 - 10: **for** i in in_the_money **do**
 - 11: **if** $inner_value[j] > continuation_values[j]$ **then**
 - 12: Set $cash_flows[i, t] = inner_value[j]$.
 - 13: Set all future cash flows for this path to 0, i.e., $cash_flows[i, (t+1) : M_E] = 0$.
 - 14: **else**
 - 15: Set $cash_flows[i, t] = 0$.
 - 16: **end if**
 - 17: $j = j + 1$.
 - 18: **end for**
 - 19: **end for**
 - 20: **end for**
 - 21: Compute the option price as the average of the discounted cash flows.
-

Parameter	Description	Value (unit)
S_0	initial stock price	36 – 44 \$
λ_0	minimum frequency of fluctuation	0.4 – 10
η	sensitivity of fluctuation in $\lambda(U_t)$	0 – 0.6
K	strike price	40 \$
μ_0	initial drift	0.06
σ	stochastic parameter	0.2
α	scaling factor	0.01
b	scaling factor	0.01
T	maturity	1
h	step size	10^{-3}
r	interest rate	0.06
M	number of paths of the asset price	10000
M_E	number of exercise points	50

Table 3: **Model parameters.** Parameters used in the LS+PDifMP algorithm.

5.3 PDifMP-based option pricing method

As an alternative to the regression-based approach of the Longstaff-Schwartz algorithm, we propose a new approach that directly employs PDifMPs to price American options. This method leverages the inherent properties of PDifMPs, in particular the random jump times, as potential exercise points for the option. In doing so, it simplifies the computational process and provides a direct mechanism for determining the option price, eliminating the need for backward iteration and regression to estimate continuation values.

The core idea of this approach is to model the asset price as a PDifMP, where the price follows a continuous path with random jumps occurring at discrete times.

These jumps, determined by the intensity function $\lambda(U_t)$ as defined in Equation (9), are treated as potential option exercise times. The flexibility of the PDifMP framework allows us to vary the number and distribution of jump times by adjusting the jump rate function $\lambda(U_t)$. This adaptability allows the model to approximate the results obtained by the Longstaff-Schwartz algorithm under different market conditions.

In this method, the intrinsic value of the option is computed at each jump time T_n . For a put option, this intrinsic value is given by $\max(K - S_{T_n}, 0)$, where K is the strike price and S_{T_n} is the asset price at time T_n . For a call option, the intrinsic value is $\max(S_{T_n} - K, 0)$. These intrinsic values are then discounted to the present value using the discount factor e^{-rT_n} , where r represents the risk-free interest rate. The final option price for each path is determined by taking the maximum of these discounted intrinsic values across all jump times along that specific path. Given M simulated paths, we let P_m denote the maximum value of the discounted intrinsic values across all possible exercise times for the

put option along the m -th path, where $m = 1, \dots, M$. This value P_m is given by

$$P_m = \max_{n=1, \dots, N} [e^{-rT_n} \max(K - S_{T_n}, 0)],$$

where e^{-rT_n} is the discount factor applied to the intrinsic value $\max(K - S_{T_n}, 0)$ at each jump time T_n , and N is the total number of jumps along the m -th path.

Similarly, for the call option, let C_m represents the maximum value of the discounted intrinsic values across all possible exercise times for the call option along the path m , such that

$$C_m = \max_{n=1, \dots, N} [e^{-rT_n} \max(S_{T_n} - K, 0)].$$

The final option price is then obtained by averaging these values across all simulated paths:

$$\text{Option Price} = \begin{cases} \frac{1}{M} \sum_{m=1}^M P_m & \text{for the put option,} \\ \frac{1}{M} \sum_{m=1}^M C_m & \text{for the call option.} \end{cases}$$

Algorithm 4 Option Pricing with PDifMP

Require: Maturity, T , strike price K , number of paths M .

- 1: Initialise an empty vector *optionValues* to store the option values for each path.
 - 2: **for** $i = 1$ to M **do**
 - 3: Use Algorithm 1 to generate a path S of the asset price with corresponding jump *times*.
 - 4: Initialise an empty vector *discountedInnerValues* to store the discounted intrinsic values.
 - 5: **for** t in *times* **do**
 - 6: Calculate the discounted intrinsic value at time t and add it to *discountedInnerValues*:
 - 7: For put option: $e^{-rt} \max(K - S_t, 0)$
 - 8: For call option: $e^{-rt} \max(S_t - K, 0)$
 - 9: **end for**
 - 10: Add the maximum of *discountedInnerValues* to *optionValues*.
 - 11: **end for**
 - 12: Output the average of *optionValues*.
-

The primary advantage of this method lies in its ability to avoid the complexities of backward iteration and regression that are inherent in the LS algorithm. By directly leveraging the jump times in PDifMPs, this approach offers a more straightforward and potentially more efficient way to price American options. However, the effectiveness of this method is heavily influenced by the choice of the jump rate function $\lambda(U_t)$. Low jump rates result in fewer exercise opportunities, which can lower the option price, while higher jump rates provide more frequent exercise opportunities, potentially raising the option price. Therefore, carefully tuning $\lambda(U_t)$ to match specific market conditions is crucial for optimising the performance of the model.

5.4 Comparative analysis of Put option pricing methods

In this section, we compare the performance of the three pricing methods—Longstaff-Schwartz (LS), Longstaff-Schwartz with PDifMP (LS+PDifMP), and the direct PDifMP method—specifically for put options. To ensure a fair and comprehensive comparison, we apply each method under the same set of initial conditions and parameters, as outlined in Table 2 and 3, respectively. The asset price paths

are simulated under identical market assumptions, with variations introduced only in the methods themselves. The strike price K and the initial asset price S_0 are fixed, while the minimum frequency λ_0 and the sensitivity parameter η are varied to explore different market conditions. The risk-free interest rate r is also held constant across all simulations. We recall the jump rate function defined as in Equation (9) (Section 3.2). In this work, we set $\beta = 0$ in Equation (9) to simplify the jump intensity function, making it directly responsive to any deviation of the asset price S_t from the reference point δ . This approach is suitable for scenarios where even small price movements relative to δ are significant. However, we recognise that in other market conditions, a non-zero β could introduce a buffer zone around δ , allowing the model to maintain a baseline jump rate λ_0 and avoid overreacting to minor fluctuations that are not critical

Therefore, the jump rate function in this context is given by

$$\lambda(U_t) := \lambda_0 + \eta \max(0, (|S_t - \delta|)),$$

and the location parameter of the Laplace distribution given by

$$a(S_t) = \mu_0 + \alpha(S_t - \delta).$$

To thoroughly evaluate their impact on option pricing, we will split the comparison into two parts. First, we will consider the case where the jump rate function and the location parameter depend on the distance between the current asset price S_t and the initial asset price S_0 , i.e. $\delta = S_0$. In this scenario, the jump rate increases as the asset price deviates from its initial value, capturing the idea that larger movements away from the starting price could indicate greater market volatility and, therefore, a higher likelihood of jumps.

Next, we will analyse the scenario where the jump rate and the location parameter are based on the distance between the current asset price S_t and the strike price K , i.e. $\delta = K$. In this case, the jump rate function is sensitive to the moneyness of the option, meaning that the probability of jumps changes as the asset price approaches or moves away from the strike price. This reflects market dynamics where significant deviations from the strike price can lead to abrupt changes in the value of the option. Under these two scenarios, we will run different sets of simulations to assess how each jump rate function influences the pricing of put options across various market conditions.

As a first step in our analysis, we fix the values of the parameters as follows: $\alpha = 10^{-6}$, $\lambda_0 = 5$, and $\eta = 0.5$. The remaining parameters are taken according to Table 3. We then compare the classic LS algorithm with the modified LS+PDifMP method for different initial asset prices S_0 . For each comparison, we consider two scenarios: one where the parameter δ is set equal to the strike price K and another where δ is set equal to the initial asset price S_0 . The results of this comparison are presented in Table 4:

S_0	δ	LS Classic	LS+PDifMP
36	40 (K)	4.472	5.450
36	36 (S_0)	4.472	4.458
38	40 (K)	3.244	4.091
38	38 (S_0)	3.244	3.264
40	40 (S_0)	2.313	2.358
42	40 (K)	1.617	1.599
42	42 (S_0)	1.617	1.681
44	40 (K)	1.118	0.933
44	44 (S_0)	1.118	1.166

Table 4: **Comparison of Put Option Prices Using LS and LS+PDifMP.** The table presents put option prices calculated using the classic LS algorithm and the modified LS+PDifMP method across various initial asset prices S_0 . The values used for the parameters are

$$\alpha = 10^{-6}, \lambda_0 = 5, \eta = 0.5.$$

The results in Table 4 highlight notable differences in the calculated put option prices between the classic LS algorithm and the LS+PDifMP method for various initial asset prices S_0 and scenarios where δ is set to either the strike price K or the initial asset price S_0 . When δ is set to K , the LS+PDifMP method generally produces higher option prices when S_0 is significantly below the strike price. This result suggests that the LS+PDifMP method is more sensitive to the likelihood of continued downward movements in the asset price, which increases the value of the put option under these conditions. However, as S_0 approaches or exceeds K , the differences diminish or even reverse, suggesting that the LS+PDifMP method adjusts for lower volatility or potential upward movements as the asset price approaches or exceeds the strike price. Conversely, when δ is set to S_0 , the LS+PDifMP method tends to produce prices very close to or slightly above those of the LS classic method, especially when S_0 is close to the strike price. This suggests that the method is sensitive to deviations from the initial asset price and provides a nuanced adjustment of the option price based on the expected volatility around S_0 . Overall, the results suggest that the LS+PDifMP method introduces valuable flexibility by varying the jump rate based on proximity to either the strike price or the initial asset price, potentially offering a more accurate reflection of market dynamics, although the effectiveness of this approach is highly dependent on the choice of δ and the specific market conditions being modelled.

Next, we fix δ to S_0 and conduct a series of experiments to further explore the performance of the LS+PDifMP method and PDifMP method compared to the classic LS algorithm under various conditions.

- **Experiment A.1:** We set $\alpha = 0.01$ and $\eta = 0$, and then compare the LS algorithm with the LS+PDifMP and the PDifMP method across different values of S_0 and λ_0 .
- **Experiment A.2:** We set $\alpha = -0.01$ and $\eta = 0$, and similarly compare the LS algorithm with the LS+PDifMP and the PDifMP method for different values of S_0 and λ_0 .
- **Experiment A.3:** We fix $\eta = 0.005$ and λ_0 , and then compare the three methods to study the effect of varying α .

In Experiment **A.1**, we set $\alpha = 0.01$ and $\eta = 0$, and compared the performance of the LS algorithm, the LS+PDifMP method, and the direct PDifMP approach across various initial asset prices S_0 and different values of the jump rate parameter λ_0 . The results are summarised in Table 5.

S_0	λ_0	Longstaff-Schwartz	LS + PDifMP	PDifMP
36	0.4	4.472	4.443	4.179
36	0.6	4.472	4.429	4.488
36	0.8	4.472	4.418	4.591
38	0.4	3.244	3.212	3.145
38	0.6	3.244	3.242	3.329
38	0.8	3.244	3.164	3.397
40	0.4	2.313	2.290	2.309
40	0.6	2.313	2.290	2.383
40	0.8	2.313	2.300	2.455
42	0.4	1.617	1.620	1.558
42	0.6	1.617	1.628	1.605
42	0.8	1.617	1.552	1.709
44	0.4	1.118	1.149	1.116*
44	0.6	1.118	1.118	1.130*
44	0.8	1.118	1.153	1.181*

Table 5: **Experiment A.1.** Put Option prices calculated using the LS, LS+PDifMP, and PDifMP methods with $\eta = 0$ and $\alpha = 0.01$, for different values of λ_0 and S_0 .

The results in Table 5 show that the put option prices obtained using the LS, LS+PDifMP and PDifMP methods are quite close, with only slight variations for different initial asset prices S_0 and jump rates λ_0 . The LS+PDifMP method is generally close to the classical LS algorithm, with only minor adjustments. The PDifMP method shows slightly more variation, especially as λ_0 increases, but the differences remain modest. Some PDifMP prices, marked with an asterisk, are based on simulations where the asset price exceeded three times its initial value, which may be unrealistic. Overall, the results suggest that the inclusion of PDifMPs leads to subtle changes in option pricing under the given conditions.

S_0	λ_0	Longstaff-Schwartz	LS + PDifMP	PDifMP
36	0.4	4.472	4.473	4.271
36	0.6	4.472	4.535	4.451
36	0.8	4.472	4.492	4.612
38	0.4	3.244	3.257	3.113
38	0.6	3.244	3.259	3.268
38	0.8	3.244	3.283	3.393
40	0.4	2.313	2.289	2.305
40	0.6	2.313	2.259	2.327
40	0.8	2.313	2.308	2.365
42	0.4	1.617	1.642	1.534
42	0.6	1.617	1.622	1.626
42	0.8	1.617	1.626	1.628
44	0.4	1.118	1.103	1.065
44	0.6	1.118	1.091	1.058
44	0.8	1.118	1.083	1.071

Table 6: **Experiment A.2.** Put Option prices calculated using the LS, LS+PDifMP, and PDifMP methods with $\eta = 0$ and $\alpha = -0.01$, for different values of λ_0 and S_0 .

The results in Table 6 show the calculated put option prices using the classic Longstaff-Schwartz (LS) algorithm, the LS+PDifMP method, and the PDifMP method for various initial asset prices S_0 and base jump rates λ_0 , with parameters $\eta = 0$ and $\alpha = -0.01$.

Compared to the previous case where $\alpha = 0.01$, the option prices in this scenario are generally similar, with only minor differences observed between the methods. The LS+PDifMP method continues to produce prices that are very close to those obtained with the LS algorithm, suggesting that the negative value of α does not significantly alter the pricing dynamics. The PDifMP method shows slightly more variation than the LS and LS+PDifMP methods, especially as λ_0 increases. However, the differences remain small. In particular, in this case, there are no option prices based on simulations where the asset price exceeded three times its initial value, which means that the potential for unrealistic pricing is not a concern here, unlike in the previous case.

S_0	α	Longstaff-Schwartz	LS + PDifMP	PDifMP
36	0.01	4.472	4.386	4.499
36	-0.01	4.472	4.449	4.540
38	0.01	3.244	3.172	3.342
38	-0.01	3.244	3.277	3.379
40	0.01	2.313	2.296	2.411
40	-0.01	2.313	2.293	2.356
42	0.01	1.617	1.623	1.691
42	-0.01	1.617	1.593	1.676
44	0.01	1.118	1.110	1.169
44	-0.01	1.118	1.105	1.133

Table 7: **Experiment A.3.** Put Option prices calculated using the LS, LS+PDifMP, and PDifMP methods with $\lambda_0 = 0.4$ and $\eta = 0.005$, for different values of α and S_0 .

Following the results of Experiments **A.1** and **A.2**, where we examined the effects of varying λ_0 and α on the pricing methods, we now focus on how different values of α affect the put option prices when λ_0 is fixed at 0.4 and η is set to 0.005. The goal of Experiment **A.3** is to determine whether adjusting the α parameter has a significant effect on option pricing and to observe how sensitive the LS+PDifMP and PDifMP methods are to changes in α . The results in table 7 show that the option prices computed by the LS, LS+PDifMP and PDifMP methods are very close over the different values of α . For all initial asset prices S_0 , the LS+PDifMP and PDifMP methods produce results that are consistent with the classic LS algorithm, suggesting that the sensitivity of these methods to the parameter α is relatively low under the given conditions. Interestingly, both the LS+PDifMP and PDifMP methods show different patterns depending on the relationship between S_0 and K . Specifically,

- Lower option prices are observed for $\alpha = 0.01$ when $S_0 < K$ and for $\alpha = -0.01$ when $S_0 > K$.
- Conversely, higher option prices are observed for $\alpha = -0.01$ when $S_0 < K$, and for $\alpha = 0.01$ when $S_0 > K$.

These patterns suggest that the direction of the adjustment factor α relative to the position of S_0 with respect to K plays a role, though subtle, in influencing the option price. Thus, Experiment **A.3** confirms that, similar to the previous experiments, the differences between the methods are subtle, indicating that all methods converge closely in their pricing of put options. Next, we conduct a series of experiments to further evaluate the performance of the LS+PDifMP and PDifMP methods compared to the classic LS algorithm under various conditions.

- **Experiment B.1:** We set α to 0.10^{-6} and 0.01 in separate runs, and then compare the LS algorithm with the LS+PDifMP method across different values of S_0 , λ_0 , and η .
- **Experiment B.2:** We fix $\eta = 0$ and examine the effect of varying λ_0 in two scenarios: one with $\alpha = 0$ and another with $\alpha = 0.01$. In both cases, we compare the LS algorithm with the PDifMP algorithm for different values of S_0 .
- **Experiment B.3:** We fix $\alpha = 0.01$ and $\lambda_0 = 0.4$, and then compare the the LS algorithm with the PDifMP algorithm to study the effect of varying η .

S_0	λ_0	η	LS classic	LS + PDifMP
36	0.5	0	4.472	4.409
36	1	0	4.472	4.451
36	0.5	0.01	4.472	4.414
38	0.5	0	3.244	3.217
38	1	0	3.244	3.205
38	0.5	0.01	3.244	3.202
40	0.5	0	2.313	2.342
40	1	0	2.313	2.289
40	0.5	0.01	2.313	2.249
42	0.5	0	1.617	1.647
42	1	0	1.617	1.677
42	0.5	0.01	1.617	1.669*
44	0.5	0	1.118	1.125
44	1	0	1.118	1.160
44	0.5	0.01	1.118	1.246*

Table 8: **Experiment B.1.** Put Option prices calculated using the LS and LS+PDifMP methods for different values of λ_0 , η , and S_0 with $\alpha = 0.01$.

In experiment **B.1**, we explore the impact of varying the parameters λ_0 and η on the put option prices calculated using the classic LS algorithm and the LS+PDifMP method. We consider two main scenarios: one with lower values of λ_0 (0.5 and 1) and η set to small values (0 and 0.01), and another with higher values of λ_0 (5 and 10) and η ranging from 0 to 0.6. The results are summarised in Tables 8 and 9.

In Table 8 from experiment **B.1**, where λ_0 is relatively low (0.5 and 1) and η is either 0 or 0.01, the LS+PDifMP method produces put option prices that are very close to those obtained with the classic LS algorithm. Similar trends are observed for other values of S_0 and λ_0 . These small differences suggest that at lower values of λ_0 and η the impact of PDifMP on pricing is minimal, indicating that the market dynamics captured by the classical LS algorithm remain largely intact even with the inclusion of PDifMP. However, at higher asset prices $S_0 = 42$ and $S_0 = 44$, with $\lambda_0 = 0.5$ and $\eta = 0.01$, the LS+PDifMP method starts to show slightly higher option prices (e.g., 1.669 and 1.246) compared to the LS algorithm (1.617 and 1.118).

S_0	λ_0	η	LS classic	LS + PDifMP
36	5	0	4.472	4.484
36	5	0.3	4.472	4.460
36	5	0.5	4.472	4.473
36	10	0.6	4.472	4.444
38	5	0	3.244	3.265
38	5	0.3	3.244	3.184
38	5	0.5	3.244	3.242
38	10	0.6	3.244	3.271
40	5	0	2.313	2.319
40	5	0.3	2.313	2.307
40	5	0.5	2.313	2.341
40	10	0.6	2.313	2.338
42	5	0	1.617	1.611
42	5	0.3	1.617	1.650
42	5	0.5	1.617	1.651
42	10	0.6	1.617	1.630
44	5	0	1.118	1.126
44	5	0.3	1.118	1.132
44	5	0.5	1.118	1.156
44	10	0.6	1.118	1.143

Table 9: **Experiment B.1.** Put Option prices calculated using the LS+PDifMP method with $\alpha = 10^{-6}$ and $\delta = S_0$, for different values of λ_0 , η , and S_0 .

Concerning the second numerical test of experiment **B.1**, where λ_0 is set to higher values (5 and 10) and η is varied more widely (0, 0.3, 0.5, 0.6), including the PDifMP in the LS algorithm has no significant effect. As shown in Table 9, for instance, when $S_0 = 36$ and $\lambda_0 = 5$, the put option price calculated by the LS+PDifMP method remains nearly constant as η increases from 0 to 0.5. This suggests that increasing λ_0 and η has only a minimal impact on the option price.

It is important to note that $\alpha = 10^{-6}$ was chosen deliberately to prevent excessively high asset prices, which could skew the results. Higher values of α might lead to more noticeable differences in option prices. Overall, the results of Experiment **B.1**, demonstrate that across a range of values for λ_0 and η , the LS+PDifMP method provides a close approximation to the classic LS algorithm, with only subtle variations in the computed put option prices. This suggests that the inclusion of PDifMP does not significantly alter the pricing outcomes under the conditions tested.

S_0	λ_0	Longstaff-Schwartz	LS + PDifMP	PDifMP
36	0.4	4.472	4.459	4.251
36	0.6	4.472	4.481	4.480
36	0.8	4.472	4.446	4.510
38	0.4	3.244	3.287	3.125
38	0.6	3.244	3.272	3.283
38	0.8	3.244	3.266	3.370
40	0.4	2.313	2.341	2.275
40	0.6	2.313	2.327	2.332
40	0.8	2.313	2.337	2.445
42	0.4	1.617	1.659	1.576
42	0.6	1.617	1.610	1.629
42	0.8	1.617	1.658	1.642
44	0.4	1.118	1.099	1.027
44	0.6	1.118	1.106	1.100
44	0.8	1.118	1.128	1.130

Table 10: **Experiment B.2.** Put Option prices calculated using the LS, LS+PDifMP, and PDifMP methods with $\eta = 0$ and $\alpha = 0$, for different values of λ_0 and S_0 .

In Experiment **B.2**, we examine the effects of varying λ_0 on put option prices calculated using the classic LS algorithm, the LS+PDifMP method, and the PDifMP method under two different settings: one with $\eta = 0$ and $\alpha = 0$, and another where we compare the LS algorithm directly with the PDifMP method for $\eta = 0$ and $\alpha = 0.01$. The results are presented in tables 10 and 11.

In the first part of Experiment **B.2**, where $\eta = 0$ and $\alpha = 0$, Table 10 shows that, overall, the option prices generated by the LS+PDifMP and PDifMP methods are comparable to those generated by the classic LS algorithm, especially as λ_0 increases from 0.4 to 0.8. For example, for $S_0 = 36$, the LS+PDifMP prices range from 4.446 to 4.481, close to the LS price of 4.472. In particular, the PDifMP method tends to produce slightly lower prices for certain values of λ_0 , but as λ_0 increases, the PDifMP prices sometimes exceed those produced by the LS and LS+PDifMP methods. This suggests that the influence of λ_0 on pricing is more significant than the initial asset price S_0 , as the price differences between methods are driven by changes in λ_0 rather than S_0 itself. These results suggest that while the PDifMP and LS+PDifMP methods introduce subtle adjustments to classical LS pricing, the overall impact remains moderate, particularly when η and α are set to zero.

S_0	λ_0	Longstaff-Schwartz	LS+PDifMP	PDifMP
32	0.4	7.967	7.952	7.116
32	0.6	7.967	7.944	7.320
32	0.8	7.967	7.960	7.596
32	1	7.967	7.961	7.784
32	1.2	7.967	7.947	7.947
34	0.4	6.043	6.011	5.605
34	0.6	6.043	6.049	5.840
34	0.8	6.043	6.010	5.958
34	1	6.043	6.020	6.142
34	1.2	6.043	6.018	6.272
46	0.4	0.740	0.760	0.770
46	0.6	0.740	0.769	0.789
46	0.8	0.740	0.815	0.824
48	0.4	0.498	0.510	0.509
48	0.6	0.498	0.513	0.554
48	0.8	0.498	0.547	0.541

Table 11: **Experiment B.2.** Put Option prices calculated using the LS and PDifMP methods with $\eta = 0$ and $\alpha = 0.01$, for different values of λ_0 and S_0 .

Table 11 compares put option prices calculated using the classic LS algorithm and the PDifMP method for various initial asset prices S_0 and base jump rates λ_0 , with $\eta = 0$. Overall, the PDifMP method tends to produce slightly lower option prices than the LS algorithm at lower S_0 values, particularly when λ_0 is low, indicating a more conservative pricing approach. As λ_0 increases, the gap between the two methods narrows, with PDifMP prices approaching or slightly exceeding LS prices, particularly at higher S_0 values. This trend suggests that as λ_0 increases, the number of potential exercise points also increases, which leads to higher option prices due to the greater likelihood of capturing advantageous price movements. The PDifMP method, in this context, becomes more sensitive to the potential for price jumps, resulting in higher option prices that reflect the increased volatility. At higher S_0 values, the differences between the methods are minimal, further highlighting the nuanced adjustments made by the PDifMP method under varying market conditions.

S_0	η	Longstaff-Schwartz	LS+PDifMP	PDifMP
36	0.001	4.472	4.415	4.353
36	0.005	4.472	4.395	4.420
36	0.01	4.472	4.334	4.728
38	0.001	3.244	3.219	3.158
38	0.005	3.244	3.241	3.332
38	0.01	3.244	3.175	3.534
40	0.001	2.313	2.322	2.304
40	0.005	2.313	2.292	2.377
40	0.01	2.313	2.272	2.516
42	0.001	1.617	1.624	1.582
42	0.005	1.617	1.631	1.683
42	0.01	1.617	1.664	1.731
44	0.001	1.118	1.154	1.163
44	0.005	1.118	1.118	1.173
44	0.01	1.118	1.186	1.201

Table 12: **Experiment B.3.** Put Option prices calculated using the LS and PDifMP methods with $\lambda_0 = 0.4$ and $\alpha = 0.01$, for different values of η and S_0 .

The results of experiment **B.3**, shown in Table 12, present put option prices computed using the classical LS algorithm and the PDifMP method for different initial asset prices S_0 and different values of the jump intensity parameter η , where $\lambda_0 = 0.4$. As η increases, the PDifMP method consistently produces higher option prices than the LS algorithm. For example, for $S_0 = 36$ \$, the PDifMP price increases from 4.353 to 4.728 as η increases from 0.001 to 0.01, indicating the sensitivity of the method to the increase in potential exercise times due to higher jump intensity. This trend is consistent across all values of S_0 , with more pronounced differences observed at higher levels of η . For instance, for $S_0 = 38$ \$, the PDifMP price increases from 3.158 to 3.534 as η increases. This suggests that the PDifMP method effectively accounts for the increased frequency of potential exercise opportunities, leading to higher option valuations as the jump intensity coefficient, represented by η , increases.

Before moving on to the analysis of call option pricing methods, we briefly examine the computational efficiency of the various methods examined in the previous sections. Table 13 shows the running times for the LS algorithm, the LS+PDifMP method and the PDifMP method for different values of the jump intensity parameter λ_0 , with fixed parameters $\alpha = 0.01$, $\eta = 0$ and an initial asset price $S_0 = 36$ \$.

λ_0	LS	LS+PDifMP	PDifMP
0.4	11.49	16.1	8.35
0.6	11.49	17.17	6.91
0.8	11.49	15.09	6.6

Table 13: **Computational Efficiency.** Comparison of the computation time (in seconds) per trial between the LS, LS+PDifMP, and PDifMP methods with parameters $\alpha = 0.01$, $\eta = 0$, and $S_0 = 36$ \$.

The results show that the PDifMP method is the most computationally efficient, with the shortest computation times over all values of λ_0 . The LS+PDifMP method takes longer due to the added complexity of modelling jumps, while the LS algorithm remains stable but slower than the PDifMP method.

5.5 Comparative analysis of Call option pricing methods

In this section, we conduct a comparative analysis of call option pricing methods using the classic LS algorithm and the PDifMP method. Similar to the approach taken for put options, we examine how varying the jump intensity parameter λ_0 affects the pricing of call options. The objective is to evaluate the performance of the PDifMP method in capturing market dynamics, particularly in scenarios where the asset price S_0 is above the strike price, which typically results in higher call option prices. This section is deliberately brief, as the primary evaluation of the PDifMP method against the LS algorithm has been thoroughly covered in the analysis of put options. The inclusion of call options here is intended to complement our findings and to provide a more comprehensive overview of the performance of the method for different types of options. In Table 14 below we present call option prices calculated using the LS and PDifMP methods for various initial asset prices S_0 and different values of λ_0 , with $\eta = 0$ and $\alpha = 0.01$.

S_0	λ_0	Longstaff-Schwartz	LS+PDifMP	PDifMP
36	0.01	2.158	2.235	2.192
36	0.1	2.158	2.181	2.215
36	0.2	2.158	2.275	2.208
38	0.01	3.171	3.216	3.174
38	0.1	3.171	3.081	3.279
38	0.2	3.171	3.293	3.292
40	0.01	4.387	4.441	4.361
40	0.1	4.387	4.473	4.531
40	0.2	4.387	4.459	4.644
42	0.01	5.786	5.802	5.801
42	0.1	5.786	5.820	6.001
42	0.2	5.786	5.825	5.994
44	0.01	7.330	7.396	7.419
44	0.1	7.330	7.429	7.461
44	0.2	7.330	7.384	7.702

Table 14: **Call option prices.** Call Option prices calculated using the LS, LS+PDifMP and PDifMP methods with $\eta = 0$ and $\alpha = 0.01$, for different values of λ_0 and S_0 .

The results in Table 14 shows that as the jump intensity parameter λ_0 increases, the call option prices calculated using the PDifMP method generally increase as well. This suggests that the PDifMP method is more responsive to changes in jump intensity and captures the potential for larger upward price movements, which are particularly relevant for call options.

At lower initial asset prices ($S_0 = 36$ \$), the differences between the LS and PDifMP methods are minimal, with PDifMP prices slightly higher than those from the LS algorithm as λ_0 increases. For example, at $\lambda_0 = 0.2$, the PDifMP method yields a price of 2.227 compared to 2.158 from the LS algorithm, reflecting a subtle adjustment for increased market volatility. As S_0 increases, the PDifMP

method continues to produce higher call option prices, particularly at higher values of λ_0 . For example, at $S_0 = 44$, the PDifMP price increases from 7.220 to 7.643 as λ_0 increases from 0.01 to 0.2. This trend is consistent with the expectation that higher jump intensities lead to higher potential payoffs for call options, which the PDifMP method effectively captures.

Overall, the results suggest that the PDifMP method provides a more nuanced reflection of market conditions by adjusting call option prices in response to changes in jump intensity, while the LS algorithm remains less sensitive to this dynamic. This responsiveness of the PDifMP method may make it a more accurate tool for pricing call options in markets characterised by high volatility and the potential for abrupt price movements.

Here, we present again the computation times for the LS, LS+PDifMP, and PDifMP methods when pricing call options with different values of λ_0 , while keeping $\alpha = 0.01$, $\eta = 0$, and $S_0 = 36$ \$. The results are shown in Table 15.

λ_0	LS	LS+PDifMP	PDifMP
0.01	3.95	105.72	109.47
0.1	3.95	16	15.66
0.2	3.95	11.72	10.49

Table 15: **Computational Efficiency.** Comparison of the computation time (in seconds) per trial between the LS, LS+PDifMP, and PDifMP methods with parameters $\alpha = 0.01$, $\eta = 0$, and $S_0 = 36$ \$.

The computation time is highest at $\lambda_0 = 0.01$, reaching 105.72 seconds for the LS+PDifMP method and 109.47 seconds for the PDifMP method. However, as λ_0 increases, the computation time decreases significantly. At $\lambda_0 = 0.2$, the time drops to 11.72 seconds for the LS+PDifMP method and 10.49 seconds for the PDifMP method. For the pricing of call options, both methods become more efficient as λ_0 increases, with the PDifMP method generally providing shorter computation times.

To further investigate the computational efficiency of the LS and PDifMP methods in call option pricing, we conducted an additional set of experiments comparing the two methods across a range of λ_0 values. Given that the previous results indicated the LS method was more efficient at lower λ_0 values, we wanted to see how this trend continues as λ_0 increases. The results are summarised in Table 16.

λ_0	LS	PDifMP
0.6	3.95	4.05
0.8	3.95	3.76
1	3.95	3.67
1.2	3.95	3.6

Table 16: **Computational Efficiency.** Comparison of the computation time (in seconds) per trial between the LS and the PDifMP methods with parameters $\alpha = 0.01$, $\eta = 0$, and $S_0 = 36$ \$.

As shown in the Table 16, the PDifMP method shows a decrease in computation time as λ_0 increases, starting from 4.05 seconds at $\lambda_0 = 0.6$ and dropping to 3.6 seconds at $\lambda_0 = 1.2$. This suggests that the PDifMP method becomes increasingly efficient as λ_0 increases, eventually approaching and even exceeding the efficiency of the LS method at higher λ_0 values.

Based on the results of both this table and the previous one (Table 15), it appears that there is an optimal λ_0 value at which the computational efficiency of the PDifMP method equals or exceeds that of the LS method. Identifying this optimal λ_0 may allow for a more balanced trade-off between computational efficiency and the nuanced pricing capabilities offered by the PDifMP method.

6 Discussion

In this paper, we have explored the use of the PDifMP method as an enhancement to the traditional Longstaff-Schwartz (LS) algorithm for pricing American options, with a focus on both put and call options. The primary aim was to assess whether the integration of PDifMP could offer a more refined approach to capturing market dynamics, particularly in scenarios characterised by significant volatility and sudden price movements.

Through a series of comprehensive experiments, we compared the classic LS algorithm, the LS+PDifMP method, and the PDifMP method across a range of market conditions, varying key parameters such as jump intensity λ_0 , initial asset price S_0 , and other model variables. Our results showed that while the differences in option prices produced by the LS, LS+PDifMP and PDifMP methods were generally modest, the LS+PDifMP method demonstrated a clear potential to adjust pricing based on jump dynamics more effectively than the traditional LS approach. This capability makes the LS+PDifMP method particularly valuable in volatile markets where capturing the full extent of price fluctuations is critical.

In addition, the PDifMP method alone demonstrated its robustness as an alternative to the LS algorithm, offering similar benefits to the LS+PDifMP method but with a simpler computational process. The PDifMP method eliminates the need for backward iteration, simplifying the computation and potentially making it more efficient in certain scenarios where computational efficiency is a priority. However, it is important to note that the PDifMP method may not always be the most efficient choice, depending on the parameter settings. This highlights the flexibility and efficiency of the method, but also emphasises the need for careful consideration of parameter selection to ensure optimal performance.

Moreover, the sensitivity of the PDifMP method to the jump intensity parameter λ_0 and the asset price S_0 suggests that it can provide more accurate pricing in markets where traditional models may fall short. The comparative analysis of call options further supports these findings, showing that the PDifMP method consistently responds to variations in market conditions, providing a comprehensive and flexible alternative to the LS algorithm.

In conclusion, the integration of PDifMP into the option pricing framework enhances the robustness of pricing models, particularly in complex and unpredictable market environments. This study provides a foundation for further research into the application of PDifMP and similar methods in financial modelling, with the potential to improve the accuracy and reliability of option pricing in practice. As future work, we plan to conduct a parameter estimation study to identify the best-fit values for the parameters used in our models, which will further refine the effectiveness and applicability of the PDifMP method in real-world scenarios.

Declaration of competing interest

The authors declare that they have no known competing financial interests or personal relationships that could have appeared to influence the work reported in this paper.

Funding

This work was partially supported by the Austrian Science Fund (FWF): W1214-N15, project DK14, as well as by the strategic program "Innovatives OÖ 2010 plus" by the Upper Austrian Government.

References

- [1] Iñigo Arregui et al. “PDE models for American options with counterparty risk and two stochastic factors: Mathematical analysis and numerical solution”. In: *Computers & Mathematics with Applications* 79.5 (2020), pp. 1525–1542.
- [2] Julien Bect. “Processus de Markov diffusifs par morceaux: outils analytiques et numériques”. PhD thesis. Université Paris Sud-Paris XI, 2007.
- [3] Howard C Berg and Douglas A Brown. “Chemotaxis in Escherichia Coli analysed by three-dimensional tracking”. In: *Nature* 239.5374 (1972), pp. 500–504.
- [4] Fisher Black and Myron Scholes. “The Pricing of Options and Corporate Liabilities”. In: *Journal of Political Economy* 81.3 (1973), pp. 637–654.
- [5] HAP Blom. “From piecewise deterministic to piecewise diffusion Markov processes”. In: *Proceedings of the 27th IEEE Conference on Decision and Control*. IEEE, 1988, pp. 1978–1983.
- [6] Phelim P Boyle. “Options: A monte carlo approach”. In: *Journal of financial economics* 4.3 (1977), pp. 323–338.
- [7] Michael J Brennan and Eduardo S Schwartz. “Finite difference methods and jump processes arising in the pricing of contingent claims: A synthesis”. In: *Journal of Financial and Quantitative Analysis* 13.3 (1978), pp. 461–474.
- [8] Mark Broadie and Paul Glasserman. “Pricing American-style securities using simulation”. In: *Journal of economic dynamics and control* 21.8-9 (1997), pp. 1323–1352.
- [9] Evelyn Buckwar and Amira Meddah. “Numerical Approximations and Convergence Analysis of Piecewise Diffusion Markov Processes, with Application to Glioma Cell Migration”. In: *arXiv preprint arXiv:2401.13428* (2024).
- [10] Evelyn Buckwar and Martin G Riedler. “An exact stochastic hybrid model of excitable membranes including spatio-temporal evolution”. In: *Journal of mathematical biology* 63.6 (2011), pp. 1051–1093.
- [11] Manuela L Bujorianu and John Lygeros. “Reachability questions in piecewise deterministic Markov processes”. In: *International Workshop on Hybrid Systems: Computation and Control*. Springer, 2003, pp. 126–140.
- [12] Manuela L Bujorianu and John Lygeros. “Toward a general theory of stochastic hybrid systems”. In: *Stochastic hybrid systems*. Springer, 2006, pp. 3–30.
- [13] Russel E Caffisch and Suneal Chaudhary. “Monte Carlo simulation for American options”. In: *A Celebration of Mathematical Modeling: The Joseph B. Keller Anniversary Volume* (2004), pp. 1–16.
- [14] Peter Carr et al. “The fine structure of asset returns: An empirical investigation”. In: *The journal of Business* 75.2 (2002), pp. 305–332.
- [15] Bertrand Cloez et al. “Probabilistic and piecewise deterministic models in biology”. In: *ESAIM: Proceedings and Surveys* 60 (2017), pp. 225–245.
- [16] John C Cox, Stephen A Ross, and Mark Rubinstein. “Option pricing: A simplified approach”. In: *Journal of financial Economics* 7.3 (1979), pp. 229–263.

- [17] Mark HA Davis. “Piecewise-deterministic Markov processes: A general class of non-diffusion stochastic models”. In: *Journal of the Royal Statistical Society: Series B (Methodological)* 46.3 (1984), pp. 353–376.
- [18] Michael C Fu et al. “Pricing American options: A comparison of Monte Carlo simulation approaches”. In: *Journal of Computational Finance* 4.3 (2001), pp. 39–88.
- [19] Steven L Heston. “A closed-form solution for options with stochastic volatility with applications to bond and currency options”. In: *The review of financial studies* 6.2 (1993), pp. 327–343.
- [20] John Hull and Alan White. “The use of the control variate technique in option pricing”. In: *Journal of Financial and Quantitative analysis* 23.3 (1988), pp. 237–251.
- [21] Hiroshi Ishijima and Masaki Uchida. “The regime switching portfolios”. In: *Asia-Pacific Financial Markets* 18 (2011), pp. 167–189.
- [22] Patrick Jaillet, Damien Lamberton, and Bernard Lapeyre. “Variational inequalities and the pricing of American options”. In: *Acta Applicandae Mathematica* 21 (1990), pp. 263–289.
- [23] Steven G Kou. “A jump-diffusion model for option pricing”. In: *Management science* 48.8 (2002), pp. 1086–1101.
- [24] Francis A. Longstaff and Eduardo S. Schwartz. “Valuing American options by simulation: a simple least-squares approach”. In: *The Review of Financial Studies* 14.1 (2001), pp. 113–147.
- [25] Amira Meddah, Martina Conte, and Evelyn Buckwar. “A stochastic hierarchical model for low grade glioma evolution”. In: *Journal of Mathematical Biology* (2023).
- [26] Robert C Merton. “Option pricing when underlying stock returns are discontinuous”. In: *Journal of financial economics* 3.1-2 (1976), pp. 125–144.
- [27] Robert C Merton. “Theory of rational option pricing”. In: *The Bell Journal of economics and management science* (1973), pp. 141–183.
- [28] Nguepedja Nankep et al. “Modélisation stochastique de systemes biologiques multi-échelles et inhomogenes en espace”. PhD thesis. Rennes, École normale supérieure, 2018.
- [29] Khashayar Pakdaman, Michele Thieullen, and Gilles Wainrib. “Fluid limit theorems for stochastic hybrid systems with application to neuron models”. In: *Advances in Applied Probability* 42.3 (2010), pp. 761–794.
- [30] Abhyudai Singh and Joao P Hespanha. “Stochastic hybrid systems for studying biochemical processes”. In: *Philosophical Transactions of the Royal Society A: Mathematical, Physical and Engineering Sciences* 368.1930 (2010), pp. 4995–5011.
- [31] Jari Toivanen. “Numerical valuation of European and American options under Kou’s jump-diffusion model”. In: *SIAM Journal on Scientific Computing* 30.4 (2008), pp. 1949–1970.